JBC Papers in Press. Published on January 14, 2002 as Manuscript M108938200

Bupivacaine Myotoxicity is Mediated by Mitochondria*

William Irwin‡, Eric Fontaine‡§, Laura Agnolucci‡, Daniele Penzo‡, Romeo Betto¶, Susan Bortolotto‡‡, Carlo Reggiani‡‡, Giovanni Salviati‡ ¶ §§ and Paolo Bernardi‡ ¶¶ //

From the Departments of ‡Biomedical Sciences and ‡‡Anatomy and Physiology, University of Padova and the Consiglio Nazionale delle Ricerche Units for the Study of ¶Muscle Pathophysiology and ¶¶Biomembranes, Viale Giuseppe Colombo 3, I-35121 Padova, Italy and the §Laboratoire de Bioénergétique Fondamentale et Appliquée, Université J. Fourier, F-38041 Grenoble, France

Proofs to be sent to:

Prof. Paolo Bernardi
Dipartimento di Scienze Biomediche Sperimentali
Viale Giuseppe Colombo 3
I-35121 Padova
Italy

Phone +39 049 827 6365
Fax +39 049 827 6361
E-mail: bernardi@bio.unipd.it

Running title: Mitochondrial Bupivacaine Myotoxicity

FOOTNOTES

*This work was supported by Grants from Telethon-Italy (Grants 847 and 1141 to P.B.), the Consiglio Nazionale delle Ricerche (Dotazione Centri Biomembrane e Fisiopatologia Muscolare). W.I. and D.P. were supported by Fellowships from Telethon-Italy and E.F. was supported by the European Economic Community Fellowship ERBFMBICT961385.

§§Deceased March 12, 1998

//To whom correspondence should be addressed: Dipartimento di Scienze Biomediche Sperimentali, Viale Giuseppe Colombo 3, I-35121 Padova, Italy

[1]The abbreviations used are:

PTP, Mitochondrial Permeability Transition Pore; CsA, Cyclosporin A; FDB, *Flexor Digitorum Brevis*; EDL, *Extensor Digitorum Longus*; PN, pyridine nucleotides; EGTA, ethylene-bis(oxoethylenenitrilo) tetraacetic acid; BSA, bovine serum albumin; FCCP, carbonylcyanide-p-trifluoromethoxyphenyl hydrazone; TMRM, tetramethyl rhodamine methyl ester; Rh123, Rhodamine 123; $\Delta\psi$, mitochondrial membrane potential difference; LI, Localization Index; BAPTA, 1,2-bis-(2-Aminophenoxy)ethane-N,N,N'N'-tetraacetic acid; MHC, Myosin heavy chain.

We have investigated the effects of the myotoxic local anesthetic bupivacaine on rat skeletal muscle mitochondria and isolated myofibers from *flexor digitorum brevis* (FDB), *extensor digitorum longus* (EDL), soleus and from the proximal, striated portion of the esophagus. In isolated mitochondria, bupivacaine caused a concentration-dependent mitochondrial depolarization and pyridine nucleotide oxidation, which were matched by an increased oxygen consumption at bupivacaine concentrations of 1.5 mM or less at pH 7.4, while respiration was inhibited at higher concentrations. As a consequence of depolarization, bupivacaine caused opening of the permeability transition pore (PTP), a cyclosporin A-sensitive inner membrane channel that plays a key role in many forms of cell death. In intact FDB fibers bupivacaine caused mitochondrial depolarization and pyridine nucleotides oxidation that were matched by increased concentrations of cytosolic free Ca^{2+}, release of cytochrome *c* and eventually hypercontracture. Both mitochondrial depolarization and cytochrome *c* release were inhibited by cyclosporin A, indicating that PTP opening rather than bupivacaine as such was responsible for these events. Similar responses to bupivacaine were observed in the soleus, which is highly oxidative. In contrast, fibers from the esophagus (which we show to be more fatiguable than FDB fibers), and from the highly glycolytic EDL didn't undergo pyridine nucleotide oxidation upon the addition of bupivacaine, and were resistant to bupivacaine toxicity. These results suggest that active oxidative metabolism is a key determinant in bupivacaine toxicity; that bupivacaine myotoxicity is a relevant model of mitochondrial dysfunction involving the PTP and Ca^{2+} dysregulation; and that it represents a promising system to test new PTP inhibitors that may prove relevant in spontaneous myopathies where mitochondria have long been suspected to play a role.

Bupivacaine is a local anesthetic that induces rapid degeneration of skeletal muscle fibers (1,2). As is the case for muscular dystrophies, the pathogenesis of bupivacaine-induced muscle cell death remains unclear. Solving this problem is of interest for the understanding of degenerative muscular diseases because the sequence of fiber breakdown induced by bupivacaine is similar to that of progressive muscular dystrophy (3). It is also striking that the same types of muscle fibers are spared by both Duchenne muscular dystrophy and bupivacaine toxicity (4,5).

It has been suggested that bupivacaine may disrupt Ca^{2+} homeostasis *in vivo*, triggering Ca^{2+}-activated cellular death pathways that include proteolysis (4,6). This suggestion is supported by the findings (i) that bupivacaine affects sarcoplasmic reticulum function *in vitro* (3); (ii) that extracellular Ca^{2+} omission delays the morphological changes (6) and decreases the protein degradation rate (7) that are observed in isolated rat soleus muscle exposed to bupivacaine; and (iii) that bupivacaine uncouples isolated rat liver and heart mitochondria (8-12) and decreases mitochondrial membrane potential and oxygen consumption both in cultured fibroblasts (13,14) and Ehrlich tumor cells (15,16). Mitochondrial dysfunction results in ATP depletion (14) and in turn is expected to have a major impact on intracellular Ca^{2+} homeostasis (17).

The importance of mitochondria in the pathways to cell death is largely recognized even if the exact mechanism(s) in specific experimental paradigms may not be easy to identify (18). A potential mechanism is represented by opening of the PTP[1], a high conductance channel located in the inner mitochondrial membrane that can be inhibited by CsA (19). PTP opening *in vitro* leads to collapse of the protonmotive force, disruption of ionic homeostasis, mitochondrial swelling, and release of cytochrome *c* (20). This sequence of events has drawn considerable attention to the PTP as a potential effector in the pathways to cell death through at least three mechanisms, *i.e.* decreased levels of cellular ATP (21-23);

increase of cytosolic Ca^{2+} (24); and release of apoptotic factors such as cytochrome *c* (25,26), apoptosis inducing factor (27), Smac-Diablo (28) and endonuclease G (29).

With the long term goal of defining the role of mitochondria in the pathways to muscle cell death (30), we have investigated the effects of bupivacaine both on rat skeletal muscle mitochondria and on isolated mouse FDB, EDL, soleus and esophagus fibers. We found that bupivacaine causes depolarization, PN oxidation and PTP opening in isolated skeletal muscle mitochondria. Measurements on isolated FDB fibers indicated that bupivacaine also induced mitochondrial depolarization that was significantly delayed by CsA *in situ*, indicating that depolarization was due to PTP opening rather than to the uncoupling effects of bupivacaine as such. Consistent with this data, bupivacaine caused CsA-inhibitable release of cytochrome *c* *in situ*. Fibers from glycolytic, non resistant to fatigue muscles such as EDL and esophagus were instead strikingly resistant to bupivacaine toxicity, suggesting that bupivacaine toxicity selectively affects oxidative muscles. Thus, bupivacaine toxicity is a relevant model of mitochondrial dysfunction involving the PTP and Ca^{2+} dysregulation, and represents a promising system to test new PTP inhibitors that may prove relevant in spontaneous myopathies where mitochondria have long been suspected to play a role, like Duchenne's muscular dystrophy (31).

Material and Methods

Rat skeletal muscle mitochondria were prepared according to (32) with slight modifications. Albino Wistars rats weighing 250-350 g were killed by decapitation and the gastrocnemius muscles were rapidly excised and transferred into the isolation medium (150 mM sucrose, 75 mM KCl, 50 mM Tris-HCl, 1 mM KH_2PO_4, 5 mM $MgCl_2$, 1 mM EGTA, pH 7.4). Muscles were minced with scissors and trimmed clean of visible fat and connective tissues. Muscle pieces were transferred to 30 ml of isolation medium supplemented with 0.2%

BSA and 0.2 mg x ml^{-1} Nagarse (Fluka, Buchs). After 1 minute, muscles were homogenized using a motor-driven Plexiglas/Plexiglas potter, transferred to 120 ml of isolation medium supplemented with 0.2% BSA and centrifuged at 700 x *g* for 10 min. The supernatant was decanted and centrifuged at 10,000 x *g* for 10 min. The resulting pellet was resuspended in a medium containing 250 mM sucrose, 0.1 mM EGTA-Tris, 10 mM Tris-HCl, pH 7.4 and centrifuged at 7,000 x *g* for 6 min. The final mitochondrial pellet was resuspended in 0.5 ml of the same medium at a final protein concentration of about 20 mg x ml^{-1}. All procedures were carried out at 0-4 °C.

Mitochondrial oxygen consumption was measured polarographically at 25 °C using a Clark-type electrode. Measurements of membrane potential and PN oxidation-reduction status were carried out fluorimetrically with a Perkin-Elmer 650-40 spectrofluorimeter equipped with magnetic stirring and thermostatic control. Membrane potential was measured in the presence of 0.1 μM Rh123 as described (33)(excitation-emission: 548-573 nm). The PN oxidation-reduction status was evaluated based on endogenous NAD(P)H fluorescence (excitation-emission: 345-450 nm).

Isolated muscle fibers were prepared from FDB, EDL, soleus muscle and from the upper region of the esophagus of C57BL/10ScSn mice according to (34) with slight modifications. Mice were killed by cervical dislocation and the muscles were incubated for 1h at 4°C in Tyrode solution containing 135 mM NaCl, 4 mM KCl, 1 mM $CaCl_2$, 1 mM $MgCl_2$, 0.33 mM KH_2PO_4, 10 mM glucose and 10 mM Hepes (pH 7.3) supplemented with 0.3% collagenase type I and 0.2% BSA. The temperature was raised to 37°C and the incubation continued for a further one hour. The muscle mass was then removed and washed twice in Tyrode solution, and single myocytes were dispersed by passing the muscle repeatedly through a wide-pore Pasteur pipette. Myocytes suspended in Tyrode solution were plated on glass coverslips and allowed to attach for at least 1 hour prior to experiment. Myocytes were

then rinsed and placed in 1 ml Tyrode solution and loaded with the indicated concentrations of TMRM for 20 min at 37 °C. Myocytes were then placed on the stage of the confocal microscope, maintaining temperature at 37 °C. In some experiments, myocytes were also loaded with 2 μM Fluo-3-AM.

Imaging was performed with either a real time confocal system (Nikon, RCM 8000) on a Nikon Diaphot-300 microscope with a 40X, 1.3 NA oil immersion objective or on a Zeiss Axiovert 100TV inverted fluorescence microscope. For the Nikon setup excitation wavelength/detection filter were 488/525 ± 25 nm bandpass and 568/585 longpass for Fluo-3 and TMRM, respectively. In some experiments, Fluo-3 and TMRM fluorescence emissions were collected simultaneously by using two separate color channels on the detector assembly. In most of the experiments sequential confocal images were acquired and stored typically at 60 sec intervals during 20-45 min. Time course of $\Delta\psi$ and $[Ca^{2+}]$ (measured in arbitrary fluorescence units) were performed using the Nikon RCM8000 Real Time Confocal System data acquisition software. Skeletal fibers were identified as regions of interest, and background was identified as an area without cells. For the Zeiss setup, a 10x objective was used. TMRM was excited with 546 ± 5 nm and the emission was monitored at 580 ± 15 nm with a 560 nm dichroic mirror. NAD(P)H was excited at 365 ± 15 nm and the emission was monitored at 460 ± 25 nm. The data was analyzed with the MetaMorph MetaFluor Imaging Software.

Cytochrome *c* release was monitored exactly as described in (35). FDB fibers were treated with vehicle or with 1 mM bupivacaine as specified in the legend to Fig. 8, and then washed. Fibers were fixed for 30 min at room temperature with 3.7% (v/v) ice-cold formaldehyde, permeabilized for 20 min with 0.01% (v/v) ice-cold Nonidet P-40, incubated for 15 min with a 0.5% solution of BSA and then for 15 min at 37°C with a mouse monoclonal anti-cytochrome *c* antibody (Pharmingen, CA, clone 6H2.B4) and with an affinity

purified rabbit antibody against the rat bc_1 complex (a generous gift of Prof. Roberto Bisson, Padova). Fibers were then sequentially incubated for 15 min at 37°C with TRITC-conjugated goat anti-mouse IgG and with FITC-conjugated goat anti-rabbit IgG. Cellular fluorescence images were acquired with a Nikon Eclipse E600 microscope equipped with a BioRad MRC-1024 laser scanning confocal imaging system. For cytochrome *c* and bc_1 complex detection, red and green channel images were acquired simultaneously using two separate color channels on the detector assembly of the Nikon Eclipse E600 microscope equipped with 488/522 ± 25 nm bandpass and 568/605 longpass filter settings, and a 60X, 1.4 NA oil immersion objective (Nikon). Using the BioRad LaserSharp analysis program, a set of lines was drawn across the cells and the fluorescence intensity of each pixel along the lines in both the green and the red channel was measured. The localization index, LI, is defined as the ratio of the standard deviation of the fluorescence intensity divided by the total fluorescence for each channel: $(S.D./\Sigma)_{red} / (S.D./\Sigma)_{green}$. A punctate distribution (which is typical of mitochondria) results in a higher S.D., and normalization allows correction for different fluorescence intensities in the two channels. The normal LI must be 1, which indicates that the bc_1 complex and cytochrome *c* have the same pattern of intracellular distribution. A LI < 1 indicates that the distribution of cytochrome *c* is more homogeneous than that of the bc_1 complex, i.e. that cytochrome *c* has diffused away from mitochondria (35).

Fiber typing of FDB, EDL, esophagus and soleus muscles was based on electrophoretic separation of MHC isoforms, which can be used as molecular markers of fiber type (36). Muscle samples were immersed in Laemmli solution (37) and MHC isoforms were resolved by the SDS-PAGE method as described (38). Briefly, 8% polyacrylamide slab gels containing 30% glycerol were run for 24h at 275V in the cold room (4°C). The gels were removed and stained with Coomassie Brilliant Blue G. Densitometry was performed using 1D Image Analysis Software (Kodak Digital Science).

Muscle fatigability was used as an index of their dependence on glycolytic or oxidative metabolic supply (39,40). The muscles were mounted in a myograph and perfused with oxygenated Krebs solution (temperature 20°C). The muscles were allowed to equilibrate for 10 minutes then the frequency (F_{max}) at which maximum isometric tension was obtained was identified. Fatigue was induced by repetitive stimulation at F_{max}. The muscles were stimulated to contract isometrically for 0.5 s every other second (duty cycle 25%). The ratio between the tension developed after 30 s and after 60 s of stimulation and the initial tension (time zero) was taken as a fatigue index.

Bupivacaine and collagenase were purchased from Sigma; Rh123, TMRM and Fluo-3 AM were purchased from Molecular Probes; and CsA was a gift from Novartis (Basel, Switzerland). All other chemicals were of the highest purity commercially available.

Results

Effects of bupivacaine on rat skeletal muscle mitochondria. Bupivacaine is an uncoupler in isolated liver and heart mitochondria (8), and causes complex effects on respiration in cultured cells (13-16). The PTP is a voltage-dependent channel that can be opened by depolarization with uncouplers and respiratory inhibitors (41). We have therefore first characterized the effects of bupivacaine on rat skeletal muscle mitochondria in the presence of CsA (in order to prevent PTP opening). The experiments of Fig. 1 document a biphasic effect of bupivacaine on the rate of oxygen consumption and on the PN oxidation-reduction status. Respiration increased linearly up to a concentration of about 1.5 mM bupivacaine and it then declined as the concentration was increased further (Fig. 1, triangles). The reduction levels of PN were a mirror image of the respiratory changes, with increased oxidation matching uncoupling and increased reduction matching respiratory inhibition (Fig. 1, squares).

Fig. 2, panel A reports the effects of increasing bupivacaine concentrations on oxygen consumption by skeletal muscle mitochondria at pH 7.4 (triangles) and pH 7.0 (squares). While the overall pattern remained biphasic, at pH 7.4 the concentrations of bupivacaine required for 50% stimulation and inhibition of respiration were approximately 0.75 and 2.2 mM, respectively. At pH 7.0 these values became approximately 1.5 mM and 4.2 mM bupivacaine, i.e. about twice the values obtained at pH 7.4. When the data were replotted as a function of the calculated concentration of the de-protonated form of bupivacaine (BP^o, pKa 8.1) it became apparent that the effects of the drug correlated with BP^o (Fig. 2, panel B). Although the pKa of bupivacaine in the membrane is not known, these findings suggest that BP^o is responsible for both uncoupling and inhibition of respiration, and indicate that the concentration of BP^o required for maximal stimulation of respiration may be as low as 0.25 mM (Fig. 2B).

We next investigated the effects of bupivacaine on the membrane potential (Fig. 3, panel A) and respiration (Fig. 3, panel B) maintained by isolated skeletal muscle mitochondria. Mitochondria were energized with complex I substrates and loaded with a small amount of Ca^{2+} in the presence of Pi, an optimal condition to reveal PTP opening by depolarization (42). It can be seen that the addition of 1 mM bupivacaine was readily followed by a fast but partial mitochondrial depolarization, followed within a few minutes by a further depolarization (panel A, trace a). These changes were matched by a transient stimulation of respiration followed by respiratory inhibition (panel B, trace a). The nature of these complex changes was elucidated when the experiment was repeated in the presence of CsA. Under these conditions, the addition of 1 mM bupivacaine was only followed by the fast, partial depolarization (panel A, trace b), while uncoupling was not followed by respiratory inhibition (panel B, trace b). Thus, both the late depolarization and the delayed inhibition of respiration were due to PTP opening. Indeed, inhibition of respiration could be

prevented by the addition of exogenous NADH (panel B, trace b) (43). Thus, by acting on three key sites of PTP regulation [*i.e.* membrane potential (41), NAD(P)H levels (44) and electron flux through complex I (33)] bupivacaine is a trigger for PTP opening in isolated skeletal muscle mitochondria.

Effects of bupivacaine on FDB mitochondria in situ. We next addressed the question of whether bupivacaine could decrease the mitochondrial membrane potential *per se* and/or through PTP opening in FDB muscle fibers. Fig. 4, panel A, shows the typical preparation used for these experiments as a fluorescence image after TMRM loading. Panel B documents that within 40 minutes of the addition of 1 mM bupivacaine the TMRM signal was largely lost while the fiber shortened considerably (panel B). The experiment of Fig. 5 illustrates the time course of the fluorescence changes of single TMRM-loaded FDB fibers elicited by the addition of 1 mM bupivacaine. The signal decreased within about 30 minutes (squares, trace a), and depolarization was prevented by CsA (closed circles, trace b) indicating that PTP opening rather than bupivacaine as such was responsible for complete depolarization under these conditions (Fig. 5). Finally, Fig. 5 shows that mitochondrial depolarization was favored by Ca^{2+}. Indeed, it could be delayed but not prevented by treatment with dantrolene, an inhibitor of Ca^{2+} release from the sarcoplasmic reticulum (triangles, trace c) or BAPTA-AM, a permeant Ca^{2+} chelator (open circles, trace d). The role of intracellular Ca^{2+} in bupivacaine toxicity was investigated further in direct measurements with the fluorescent indicator Fluo-3. The experiments of Fig. 6, panel A, show that mitochondrial depolarization induced by bupivacaine (circles, trace a) was mirrored by an increase of $[Ca^{2+}]_c$ (squares, trace b), which was observed also in nominally Ca^{2+}-free media (not shown). Fig. 6, panel B, shows that in a Ca^{2+}-free medium ryanodine was able to prevent the rise of $[Ca^{2+}]_c$ (squares, trace b) but not mitochondrial depolarization (circles, trace a). These experiments suggests that the latter is the cause rather than the consequence of dysregulation of Ca^{2+} homeostasis.

The depolarization due to the addition of bupivacaine prior to onset of PTP opening was clearly detectable in isolated mitochondria (Fig. 3A) but not in FDB fibers (Fig. 5). However, the TMRM fluorescence changes of mitochondria following depolarization *in situ* may be complex [see (45,46) for recent reviews]. We therefore also studied the changes of the oxidation-reduction state of endogenous PN, which reflects the rate of electron flux within the respiratory chain. The experiments depicted in Fig. 7 demonstrate that the addition of bupivacaine was followed by the expected oxidation of PN *in situ* (squares, trace a). As was the case for depolarization, however, also PN oxidation was inhibited by CsA (circles, trace b). These results indicate that, at this concentration, bupivacaine has little direct (i.e., PTP-independent) effects on the membrane potential.

Bupivacaine releases cytochrome c from mitochondria in FDB fibers. PTP opening plays a role in several paradigms of cell death that depend on cytochrome *c* release, which may be followed by caspase activation. We have studied whether bupivacaine causes cytochrome *c* release in FDB fibers with a very sensitive *in situ* method that was recently developed in one of our laboratories (35). The experiments of Fig. 8 report the distribution of cytochrome *c* (red) and of the bc_1 complex (green) in an untreated FDB fiber (panel A) or after 30' of treatment with 1 mM bupivacaine in the absence (panel B) or presence (panel C) of CsA. The quantitative analysis of the fluorescence pattern of the two channels (35) revealed a modest but significant difference in the distribution of cytochrome *c* after treatment with bupivacaine. This redistribution was fully prevented by CsA implying PTP opening as a causative event (panel D).

EDL and esophagus fibers are resistant to bupivacaine toxicity. Fig. 9 shows that within two minutes of the addition of 2 mM bupivacaine FDB fibers hypercontracted (panel A', compare with panel A). This event was followed by the formation of blebs in the sarcolemma and eventually by permeability changes that compromised cell viability (not

shown). Fig. 9 also shows that the same concentration of bupivacaine was ineffective at inducing contracture of striated fibers from the esophagus after 20 minutes (panel B', compare with panel B), while a modest effect was seen after 40 minutes (panel B''). Prompted by this observation, we investigated whether the myotoxic effects of bupivacaine are dependent on the fiber type.

Fig. 10 shows that addition of bupivacaine caused a deep oxidation of PN in the soleus fibers, an event that was readily followed by hypercontracture (panel A, trace a). Strikingly, the same concentration of bupivacaine was ineffective in fibers from the EDL (panel A, trace b) and from the esophagus (panel A, trace c). In order to explore whether this diversity could be traced to fiber composition we studied the pattern of MHC isoform expression, which can be used as a molecular marker of the fiber type (36). Fig. 10, panel B, shows that in the esophagus and in the EDL the predominant isoform was IIb (esophagus: 57% IIb and 43 % IIx(d); EDL: 65% Iib, 23% IIx(d) and 12% IIa) , whereas FDB expressed predominantly myosin IIa (50%) and IIx(d) (41%) with low levels of myosins IIb (5%) and I or slow (4%). By comparison soleus expressed equal amounts of IIx(d), IIa and I. Expression of IIb myosin generally associates with glycolytic metabolism, whereas expression of IIa and IIx(d) myosins associates with oxidative metabolism (47).

To further characterize the metabolic profile of the four muscles we measured resistance to fatigue, which is dependent on the ability to produce ATP with oxidative metabolism avoiding intracellular accumulation of H^+ and Pi. The fatigue index, which represents the active force still developed after a period of contractile activity, was determined after 30 s and 60 s of repetitive stimulation (see Methods). The fatigue indexes (values refer to 30 and 60 s of stimulation, respectively, and are expressed as mean ± standard error) were: 0.90 ± 0.02 and 0.84 ± 0.02 for the FDB, 0.90 ± 0.003 and 0.79 ± 0.04 for the soleus, 0.81 ± 0.01 and 0.76 ± 0.01 for the esophagus, and 0.61 ± 0.06 and 0.40 ± 0.06 for the EDL. The

higher fatigue resistance of FDB and soleus and the presence of energetically less expensive myosin isoforms (mainly IIa and IIx(d)) indicates an active oxidative metabolism. The abundance of the fast and energetically expensive myosin IIb and the glycolytic metabolism cooperate to make EDL and esophagus less resistant to fatigue.

Discussion

Multiple effects of bupivacaine on mitochondrial energy metabolism. The mechanism through which the local anesthetic bupivacaine uncouples oxidative phosphorylation has been the subject of considerable debate in Bioenergetics (8,10-12,48). This is due both to the intrinsic interest of clarifying the mechanisms of uncoupling by hydrophobic amines, which are largely used as anesthetics; and to an effort to understand the basis of bupivacaine toxicity (49,50) which is exploited to induce cell death in studies of muscle regeneration (1,2). Despite initial controversies, it appears now established that bupivacaine is a bona fide protonophore (8) although it can also form ion pairs with lipophilic anions (11,48). Since we discovered that bupivacaine can induce the PTP both in isolated mitochondria and intact muscle fibers, it was essential to preliminarly reinvestigate the effects of bupivacaine on mitochondrial energy metabolism under conditions where a contribution of the PTP itself could be excluded, a question that had not been addressed in previous studies on the mechanisms of uncoupling by bupivacaine. The issue is important because PTP opening can cause both uncoupling and respiratory inhibition through depletion of matrix PN (33). Our results with isolated mitochondria demonstrate that bupivacaine is a mitochondrial uncoupler at concentrations of the free base below 0.25 mM, while higher concentrations cause respiratory inhibition, with matching changes of the oxidation-reduction status of mitochondrial PN (Figs. 1 and 2).

The PTP-inducing effects of bupivacaine in isolated mitochondria can be explained within the framework of pore regulation by the membrane potential (41), the oxidation-

reduction state of PN (51) and the electron flux through Complex I (33). Indeed, low concentrations of bupivacaine can increase the probability of pore opening through membrane depolarization (Fig. 3A), which would synergize with NADH oxidation and increased electron flux secondary to uncoupling (Fig. 1). What remains more difficult to understand is why no measurable changes of TMRM and PN fluorescence can be detected upon addition of bupivacaine *before* onset of the permeability transition (Figs. 5-7). One possibility is that the small depolarization induced by bupivacaine is offset by an increased flux through glycolysis (15) and/or the Krebs cycle, or that glycolytic ATP can be used to sustain the membrane potential (16). This would mean that the major mechanism through which bupivacaine induces PTP opening *in situ* is through increased electron flux, which indeed is a key determinant in regulation of the PTP in skeletal muscle mitochondria (33). In any case, our results demonstrate that PTP opening is the major underlying cause of mitochondrial depolarization induced by bupivacaine in isolated FDB fibers, and that this event is essential for the subsequent dysfunction that leads to hypercontracture and cell death.

The mechanism of bupivacaine-dependent cell death. The mechanisms of bupivacaine-dependent cell death downstream of mitochondria remain unclear. It is reasonable to hypothesize that depletion of ATP and the rise of cytosolic Ca^{2+} concentration play a prominent role. Damage could then be amplified by increased production of superoxide anion following mitochondrial release of cytochrome *c* (52), and additional factors would be activation of proteases and possibly caspases. It has recently been shown that cytosols from human skeletal muscle lack the ability to activate type-II caspases despite the presence of procaspases 3 and 9, a finding that could be explained by the lack of cytosolic Apaf-1 (53). These findings have been taken to indicate that human skeletal muscle cells should be refractory to mitochondria-mediated proapoptotic events (53). We have not directly addressed whether cytochrome *c* release activates caspase 9 in FDB fibers from the mouse. However,

other proapototic factors are likely to be released when the permeability transition takes place including Apoptosis Inducing Factor (27) and endonuclease G (29), which both cause nuclear degradation independent of caspase activation.

Our experiments have shown that the oxidative FDB and soleus fibers are very sensitive to bupivacaine toxicity while the glycolytic EDL and esophagus fibers are strikingly resistant. Like the EDL, esophagus fibers appear to be mostly glycolytic based on both resistance to fatigue and on the prevailing myosin types. These findings therefore suggest that oxidative fibers are the main target of bupivacaine. The mechanistic basis for this striking difference is under active investigation, but these results already have interesting implications for muscle pathophysiology.

Implications for muscle pathophysiology. The structural basis of muscular dystrophies has been traced to defects of the dystrophin-glycoprotein complex linking the extracellular matrix to the cytoskeleton (54). In Duchenne's muscular dystrophy and in its mouse *mdx* model the molecular defect resides in dystrophin, while other proteins of the complex are missing or altered in other forms of muscular dystrophy (55). Although the pathogenesis remains unclear, Ca^{2+} dysregulation appears to be a key factor in disease onset and progression. This could be due to both decreased fiber resistance to mechanical stress resulting in sarcolemmal damage (56) and to increased Ca^{2+} flux through mechanosensitive channels prior to sarcolemmal damage (57). The resulting increase of cytosolic [Ca^{2+}] would cause damage by activation of proteases and/or by increased oxidative stress eventually leading to cell death (58). Specific muscles are spared by the disease, however, and these include the extraocular muscles (59) and the esophagus (60). In the case of extraocular muscle the adaptive mechanism appears to be at least in part linked to upregulation of the closely related utrophin, yet selected fibers are resistant to death even in mice lacking both dystrophin and utrophin (61). Furthermore, extraocular muscles are also spared in mice carrying the

targeted deletion of both the γ- and δ-sarcoglycan genes, a murine model of limb girdle muscular dystrophy where utrophin cannot provide compensation for the defect (62). This finding led Porter and Coworkers to contend that « the disruption of dystroglycan complex organization does not inevitably produce myofiber death but suggests that there are inherent properties of extraocular muscle that permit its protection from the dystrophic process » (62). Strikingly, both extraocular muscle (4) and esophagus fibers (Fig. 9) are resistant to bupivacaine toxicity as well. Mitochondrial dysfunction has long been suspected to be a key determinant in the biochemical events downstream of the genetic lesion of muscular dystrophy (31). It is established that Ca^{2+} overload is a key factor for mitochondrial damage (24). If mitochondria prove to be the link between Ca^{2+} dysregulation and cell death, bupivacaine toxicity may provide a model to test mitochondrial drugs of potential relevance to these diseases.

References

1. Milburn, A. (1976) *J. Neurocytol.* **5,** 425-446

2. Hall-Craggs, E. C. (1980) *Br. J. Exp. Pathol.* **61,** 139-149

3. Nonaka, I., Takagi, A., Ishiura, S., Nakase, H., and Sugita, H. (1983) *Acta Neuropathol. Berl.* **60,** 167-174

4. Porter, J. D., Edney, D. P., McMahon, E. J., and Burns, L. A. (1988) *Invest. Ophthalmol. Vis. Sci.* **29,** 163-174

5. Kaminski, H. J., al, H. M., Leigh, R. J., Katirji, M. B., and Ruff, R. L. (1992) *Ann. Neurol.* **32,** 586-588

6. Steer, J. H., Mastaglia, F. L., Papadimitriou, J. M., and Van Bruggen, I. (1986) *J. Neurol. Sci.* **73,** 205-217

7. Steer, J. H. and Mastaglia, F. L. (1986) *J. Neurol. Sci.* **75,** 343-351

8. Dabadie, P., Bendriss, P., Erny, P., and Mazat, J. P. (1987) *FEBS Lett.* **226,** 77-82

9. van Dam, K., Shinohara, Y., Unami, A., Yoshida, K., and Terada, H. (1990) *FEBS Lett.* **277,** 131-133

10. Terada, H., Shima, O., Yoshida, K., and Shinohara, Y. (1990) *J. Biol. Chem.* **265,** 7837-7842

11. Sun, X. and Garlid, K. D. (1992) *J. Biol. Chem.* **267,** 19147-19154

12. Schönfeld, P., Sztark, F., Slimani, M., Dabadie, P., and Mazat, J. P. (1992) *FEBS Lett.* **304,** 273-276

13. Grouselle, M., Tueux, O., Dabadie, P., Georgescaud, D., and Mazat, J. P. (1990) *Biochem. J.* **271,** 269-272

14. Sztark, F., Tueux, O., Erny, P., Dabadie, P., and Mazat, J. P. (1994) *Anesth. Analg.* **78,** 335-339

15. Floridi, A., Barbieri, R., Pulselli, R., Fanciulli, M., and Arcuri, E. (1994) *Oncol. Res.* **6,** 593-601

16. Pulselli, R., Arcuri, E., Paggi, M. G., and Floridi, A. (1996) *Oncol. Res.* **8,** 267-271

17. Bernardi, P. (1999) *Physiol. Rev.* **79,** 1127-1155

18. Bernardi, P., Scorrano, L., Colonna, R., Petronilli, V., and Di Lisa F. (1999) *Eur. J. Biochem.* **264,** 687-701

19. Crompton, M. (1999) *Biochem. J.* **341,** 233-249

20. Petronilli, V., Nicolli, A., Costantini, P., Colonna, R., and Bernardi, P. (1994) *Biochim. Biophys. Acta* **1187,** 255-259

21. Imberti, R., Nieminen, A. L., Herman, B., and Lemasters, J. J. (1993) *J. Pharmacol. Exp. Ther.* **265,** 392-400

22. Pastorino, J. G., Snyder, J. W., Serroni, A., Hoek, J. B., and Farber, J. L. (1993) *J. Biol. Chem.* **268,** 13791-13798

23. Duchen, M. R., McGuinness, O., Brown, L. A., and Crompton, M. (1993) *Cardiovasc. Res.* **27,** 1790-1794

24. Duchen, M. R. (1999) *J. Physiol. Lond.* **516,** 1-17

25. Pastorino, J. G., Chen, S. T., Tafani, M., Snyder, J. W., and Farber, J. L. (1998) *J. Biol. Chem.* **273,** 7770-7775

26. Scorrano, L., Penzo, D., Petronilli, V., Pagano, F., and Bernardi, P. (2001) *J. Biol. Chem.* **276,** 12035-12040

27. Susin, S. A., Lorenzo, H. K., Zamzami, N., Marzo, I., Snow, B. E., Brothers, G. M., Mangion, J., Jacotot, E., Costantini, P., Loeffler, M., Larochette, N., Goodlett, D. R., Aebersold, R., Siderovski, D. P., Penninger, J. M., and Kroemer, G. (1999) *Nature* **397,** 441-446

28. Chai, J., Du, C., Kyin, S., Wang, X., and Shi, Y. (2000) *Nature* **406,** 855-862

29. Li, L. Y., Luo, X., and Wang, X. (2001) *Nature* **412,** 95-99

30. Bernardi, P. (1999) *Ital. J. Neurol. Sci.* **20,** 395-400

31. Wrogemann, K. and Pena, S. D. (1976) *Lancet* **1,** 672-674

32. Madsen, K., Ertbjerg, P., and Pedersen, P. K. (1996) *Anal. Biochem.* **237,** 37-41

33. Fontaine, E., Eriksson, O., Ichas, F., and Bernardi, P. (1998) *J. Biol. Chem.* **273,** 12662-12668

34. Liu, Y., Carroll, S. L., Klein, M. G., and Schneider, M. F. (1997) *Am. J. Physiol.* **272,** C1919-C1927

35. Petronilli, V., Penzo, D., Scorrano, L., Bernardi, P., and Di Lisa F. (2001) *J. Biol. Chem.* **276,** 12030-12034

36. Schiaffino, S. and Reggiani, C. (1996) *Physiol Rev.* **76,** 371-423

37. Laemmli, U. K. (1970) *Nature* **227,** 680-685

38. Talmadge, R. J. and Roy, R. R. (1993) *J. Appl. Physiol.* **75,** 2337-2340

39. Fitts, R. H. (1994) *Physiol Rev.* **74,** 49-94

40. Westerblad, H., Allen, D. G., Bruton, J. D., Andrade, F. H., and Lannergren, J. (1998) *Acta Physiol Scand.* **162,** 253-260

41. Bernardi, P. (1992) *J. Biol. Chem.* **267,** 8834-8839

42. Petronilli, V., Cola, C., and Bernardi, P. (1993) *J. Biol. Chem.* **268,** 1011-1016

43. Vinogradov, A., Scarpa, A., and Chance, B. (1972) *Arch. Biochem. Biophys.* **152,** 646-654

44. Haworth, R. A. and Hunter, D. R. (1980) *J. Membr. Biol.* **54,** 231-236

45. Nicholls, D. G. and Ward, M. W. (2000) *Trends Neurosci.* **23,** 166-174

46. Bernardi, P., Petronilli, V., Di Lisa F., and Forte, M. (2001) *Trends Biochem. Sci.* **26,** 112-117

47. Pette, D. and Staron, R. S. (1990) *Rev. Physiol Biochem. Pharmacol.* **116,** 1-76

48. Garlid, K. D. and Nakashima, R. A. (1983) *J. Biol. Chem.* **258,** 7974-7980

49. Eledjam, J. J., de la Coussaye, J. E., Brugada, J., Bassoul, B., Gagnol, J. P., Fabregat, J. R., Masse, C., and Sassine, A. (1989) *Anesth. Analg.* **69,** 732-735

50. de la Coussaye, J. E., Bassoul, B., Albat, B., Peray, P. A., Gagnol, J. P., Eledjam, J. J., and Sassine, A. (1992) *Anesth. Analg.* **74,** 698-702

51. Costantini, P., Chernyak, B. V., Petronilli, V., and Bernardi, P. (1996) *J. Biol. Chem.* **271,** 6746-6751

52. Cai, J. and Jones, D. P. (1998) *J. Biol. Chem.* **273,** 11401-11404

53. Burgess, D. H., Svensson, M., Dandrea, T., Gronlund, K., Hammarquist, F., Orrenius, S., and Cotgreave, I. A. (1999) *Cell Death Differ.* **6,** 256-261

54. Ervasti, J. M. and Campbell, K. P. (1991) *Cell* **66,** 1121-1131

55. Campbell, K. P. (1995) *Cell* **80,** 675-679

56. Mokri, B. and Engel, A. G. (1975) *Neurology* **25,** 1111-1120

57. Franco, O. A. J. and Lansman, J. B. (1994) *J. Physiol. Lond.* **481,** 299-309

58. Brown, R. H. (1995) *Curr. Opin. Neurol.* **8,** 373-378

59. Porter, J. D. and Baker, R. S. (1996) *Neurology* **46,** 30-37

60. Karpati, G. and Carpenter, S. (1986) *Am. J. Med. Genet.* **25,** 653-658

61. Porter, J. D., Rafael, J. A., Ragusa, R. J., Brueckner, J. K., Trickett, J. I., and Davies, K. E. (1998) *J. Cell Sci.* **111,** 1801-1811

62. Porter, J. D., Merriam, A. P., Hack, A. A., Andrade, F. H., and McNally, E. M. (2001) *Neuromuscul. Disord.* **11,** 197-207

Figure legends

Figure 1. Effect of bupivacaine on the oxygen consumption rate and pyridine nucleotides oxidation-reduction state of rat skeletal muscle mitochondria. The incubation medium contained 250 mM sucrose, 20 mM KCl, 10 mM K^+ phosphate, 5 mM glutamate-Tris, 5 mM pyruvate-Tris, 2.5 mM malate-Tris, and 5 mM $MgCl_2$. Final volume 2 ml, pH 7.4, 25 °C. The experiments were started by the addition of 0.6 mg of skeletal muscle mitochondria (not shown) followed by the indicated concentrations of bupivacaine, whose structure is depicted in the figure. *Triangles*, oxygen consumption; *Squares*, oxidation-reduction level of pyridine nucleotides. Values on the ordinate refer to the ratio between the respiratory rate following and preceding the addition of bupivacaine (Oxygen Utilization) or to arbitrary units (for NAD(P)H Levels). Measurements were performed in parallel incubations of the same mitochondrial preparation. For further details see the Materials and Methods Section.

Figure 2. Effects of bupivacaine on mitochondrial respiration at pH 7.4 and 7.0. *Panel A*, the experimental conditions were exactly as in Fig. 1, except that the final pH was 7.4 (triangles) or 7.0 (squares). In *panel B* the data have been replotted as a function of the calculated concentration of deprotonated bupivacaine (pKa 8.1). Values on the ordinate are as in Fig. 1.

Figure 3. Effects of bupivacaine and CsA on mitochondrial membrane potential and respiration. Skeletal muscle mitochondria (0.4 mg) were incubated in 250 mM sucrose, 10 mM Tris-MOPS, 10 mM Pi-Tris, 5 µM EGTA-Tris, 5 mM glutamate-Tris, 5 mM pyruvate-Tris, 2.5 mM malate-Tris. Final volume 2 ml, 25°C. *Panel A*, the medium was supplemented with 0.2 µM Rh123; *traces b* (both panels) 1 µM CsA was present. Where indicated 20 µM

Ca^{2+}, 1 mM bupivacaine, 2 mM NADH and 2 μM rotenone were added. *Panel A*, changes of membrane potential (Δψ), as measured from the changes of Rh123 fluorescence; *Panel B*, oxygen consumption.

Figure 4. Effect of bupivacaine on mitochondrial TMRM staining in isolated skeletal muscle fibers. The mitochondrial membrane potential of intact mouse FDB muscle fibers was monitored by TMRM fluorescence at 100X magnification in Tyrode buffer supplemented with 25 mM Hepes at pH 7.3. FDB fibers were previously loaded with 10 nM TMRM at 37° C for 10 minutes in Tyrode buffer. The figure on the right is the same FDB fiber 40 minutes after the addition of 1 mM bupivacaine, which induced the loss of mitochondrial membrane potential and hypercontracture.

Figure 5. Effects of CsA, dantrolene and BAPTA-AM on bupivacaine-dependent changes of mitochondrial TMRM fluorescence in isolated FDB muscle fibers. Experimental conditions were as in Fig. 4. In all cases, 1 mM bupivacaine was added at T = 4 minutes. Additions of CsA (2 μM, closed circles, trace b), dantrolene (0.1 mM, triangles, trace c) or BAPTA-AM (5 μM, open circles, trace d), were made at T = 0 minutes (not shown). Squares (trace a), only bupivacaine was added. Values on the ordinate refer to the normalized TMRM fluorescence signals.

Figure 6. Effect of bupivacaine on $[Ca^{2+}]_c$ and mitochondrial TMRM fluorescence in FDB fibers. The experimental conditions were as in Fig. 4. The incubation medium was complete Tyrode in Panel A, and Ca^{2+}-free Tyrode supplemented with 100 μM ryanodine in Panel B. Isolated FDB fibers were stained with 10 nM TMRM and 2 μM Fluo-3 AM, and the fluorescence of TMRM (circles, traces a) and Fluo-3 (squares, traces b) was followed over

time by laser confocal microscopy. Where indicated 2 mM bupivacaine was added. Values on the ordinate refer to the normalized TMRM or Fluo-3 fluorescence signals. In both panels an asterisk denotes onset of hypercontracture.

Figure 7. Effect of CsA on the changes of the NAD(P)H signal induced by bupivacaine in FDB Fibers. The NAD(P)H signal from single mouse FDB fibers was monitored by fluorescence microscopy in Tyrode buffer with 25 mM HEPES. Where indicated 0.5 mM bupivacaine was added at T = 5 minutes. In the experiment denoted by circles the fiber had been treated with 4 μM CsA at T = 0 minutes. Values on the ordinate refer to the normalized NAD(P)H signal. Asterisks denote onset of hypercontracture.

Figure 8. Effects of bupivacaine and CsA on cytochrome *c* distribution in FDB fibers. FDB fibers were fixed and treated with anti cytochrome *c* (red) and anti bc_1 complex antibodies (green) as described in the Materials and Methods Section. Prior to fixation, the fibers were incubated in the absence of additions (*Panel A*), or treated with 1.0 mM bupivacaine for 30 min in the absence (*Panel B*) or presence (*Panel C*) of 2 μM CsA. *Panel D* reports an analysis of the distribution of cytochrome *c* relative to the bc_1 complex carried out as described in the materials and methods section [see also (35)] after the addition of bupivacaine for the indicated periods of time in the absence (open bars) or presence (hatched bars) of 2 μM CsA. Grey bar, no bupivacaine addition. A localization index of 1.0 signifies that cytochrome *c* has the same distribution of the bc_1 complex, while an index lower than 1 means that the distribution fo cytochrome *c* is more homogenoeus than that of the bc_1 complex.

Figure 9. Effect of bupivacaine on FDB versus esophagus muscle fibers. Two FDB (*Panels A, A' and A''*) and one esophagus (*Panels B, B', B''*) muscle fibers were incubated in Tyrode buffer supplemented with 25 mM Hepes at pH 7.3 and 25° C. A set of optical transmission microscopy pictures was taken (magnification 100x) before (*Panels A and B*) and 2 minutes (*Panel A'*), 20 minutes (*Panel B'*), or 40 minutes (*Panels A'' and B''*) after the addition of 2 mM bupivacaine.

Figure 10. Responses of soleus, EDL and esophagus fibers to bupivacaine: Correlation to fiber MHC composition. *Panel A.* Soleus (closed squares, trace a), EDL (open squares, trace b) and esophagus muscle fibers (closed circles, trace c) were incubated in Tyrode buffer supplemented with 25 mM Hepes (pH 7.3). Where indicated, 1 mM (trace c) or 2 mM (traces a and b) bupivacaine and 5 μM FCCP were added. Values on the ordinate refer to the relative NAD(P)H fluorescence, and the asterisk denotes onset of fiber hypercontracture. *Panel B*. Electrophoretic separation of MHC isoforms of EDL, esophagus, FDB and soleus muscles. MHC isoforms are used as molecular markers of fiber type, and the position of the MHC isoforms is denoted by arrows.

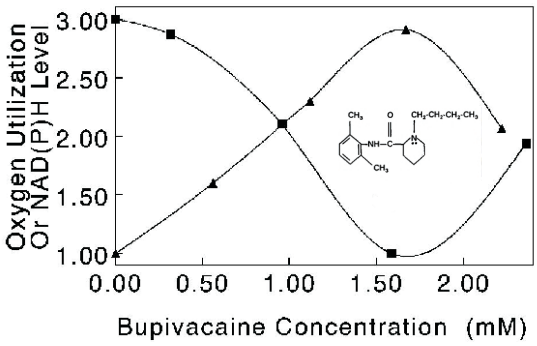

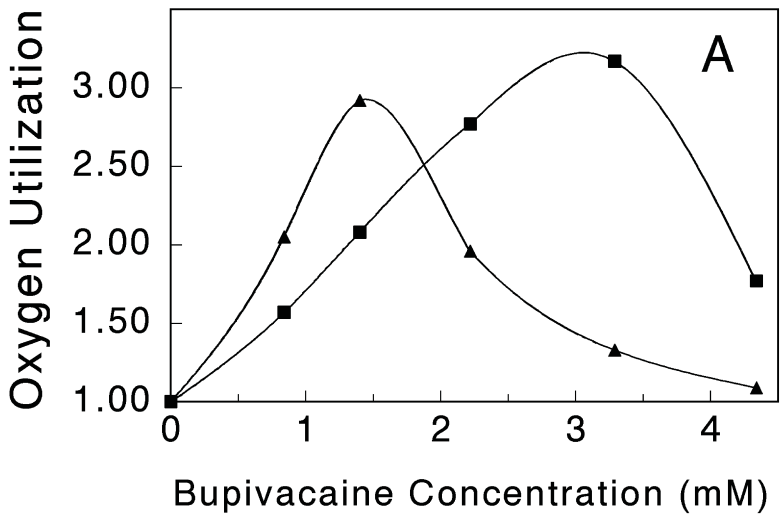

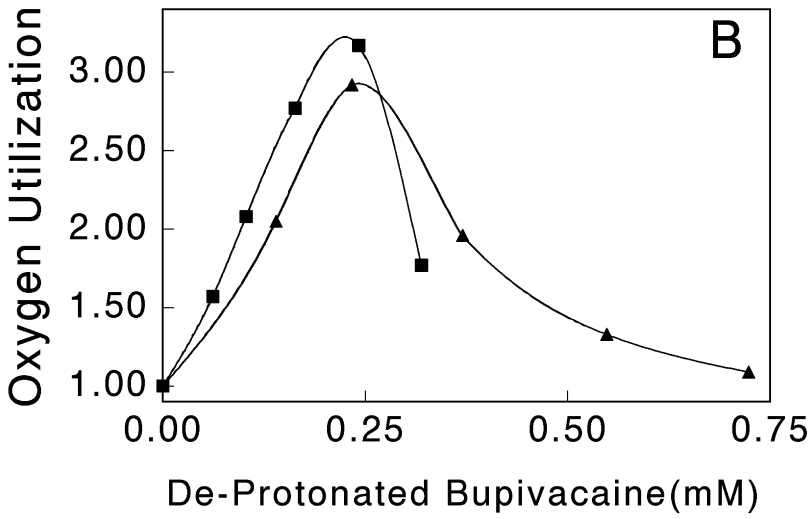

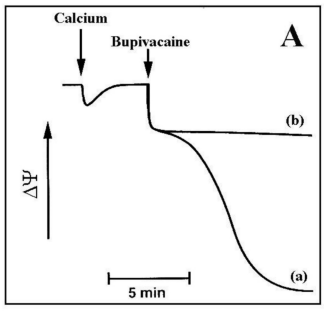

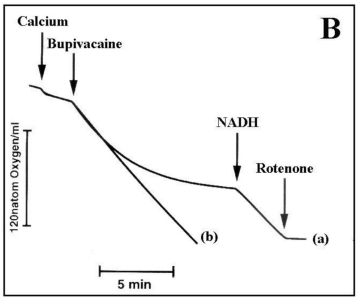

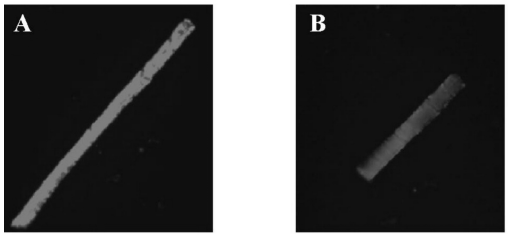

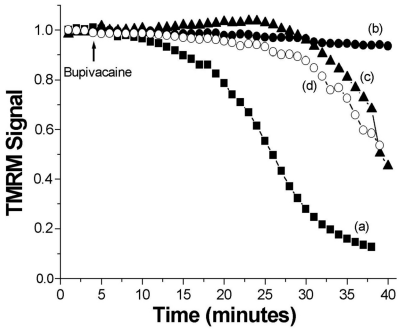

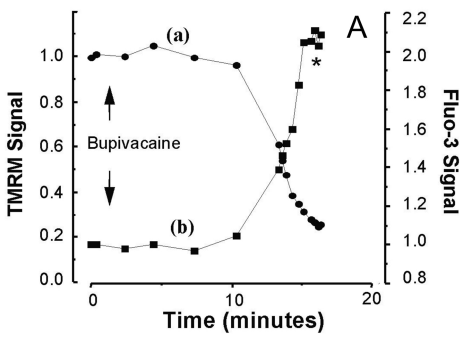

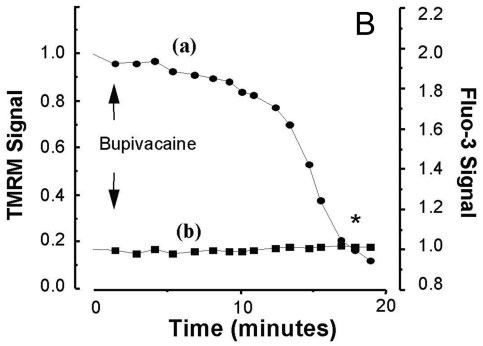

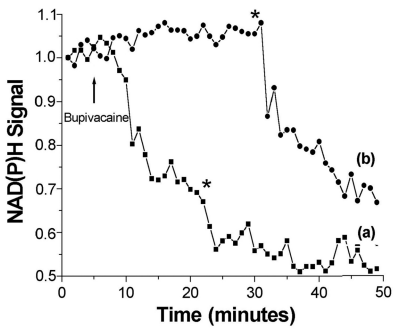

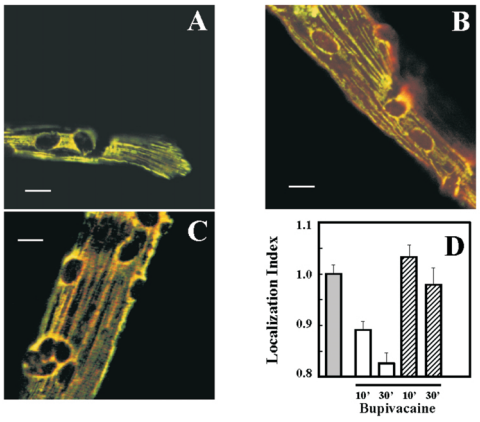

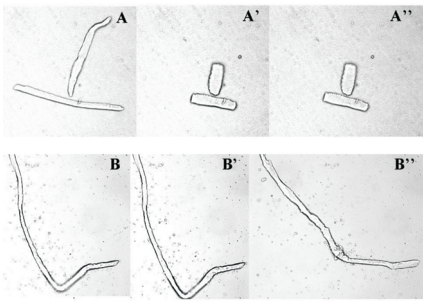

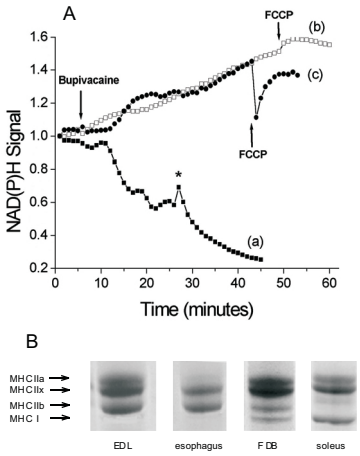

Bupivacaine myotoxicity is mediated by mitochondria

William Irwin, Eric Fontaine, Laura Agnolucci, Daniele Penzo, Romeo Betto, Susan Bortolotto, Carlo Reggiani, Giovanni Salviati and Paolo Bernardi

J. Biol. Chem. published online January 14, 2002
